Nucleotide Binding to the Multidrug Resistance P-Glycoprotein as Studied by ESR Spectroscopy†

Sabine Delannoy,§ Ina L. Urbatsch,‡ Gregory Tombline,# Alan E. Senior,# and Pia D. Vogel*,§

Department of Biological Sciences, Southern Methodist University, Dallas, Texas 75275, Cell Biology and Biochemistry, Texas Tech University Health Science Center, Lubbock, Texas 79430, and Department of Biochemistry and Biophysics, University of Rochester Medical Center, Rochester, New York 14642

Received June 28, 2005; Revised Manuscript Received August 24, 2005

ABSTRACT: Electron spin resonance (ESR) spectroscopy using spin-labeled ATP was used to study nucleotide binding to and structural transitions within the multidrug resistance P-glycoprotein, P-gp. Spin-labeled ATP (SL-ATP) with the spin label attached to the ribose, was observed to be an excellent substrate analogue for P-gp. SL-ATP was hydrolyzed in a drug-stimulated fashion at about 14% of the rate for normal ATP and allowed reversible trapping of the enzyme in transition and ground states. Equilibrium binding of a total of two nucleotides per P-gp was observed with a binding affinity of 366 μM in the presence of Mg^{2+} but in the absence of transport substrates such as verapamil. Binding of SL-ATP to wild-type P-gp in the presence of verapamil resulted in reduction of the protein-bound spin-label moiety, most likely due to a conformational transition within P-gp that positioned cysteines in close proximity to the spin label to allow chemical reduction of the radical. We circumvented this problem by using a mutant of P-gp in which all naturally occurring cysteines were substituted for alanines. Equilibrium binding of SL-ATP to this mutant P-gp resulted in maximum binding of two nucleotides; the binding affinity was 223 μM in the absence and 180 μM in the presence of verapamil. The corresponding ESR spectra of wild-type and Cys-less P-gp in the presence of SL-ATP indicate that a cysteine side chain of P-gp is located close to the ribose of the bound nucleotide. Trapping SL-ATP as an AlF_x-adduct resulted in ESR spectra that showed strong immobilization of the radical, supporting the formation of a closed conformation of P-gp in its transition state. This study is the first to employ ESR spectroscopy with the use of spin-labeled nucleotide analogues to study P-glycoprotein. The study shows that SL-ATP is an excellent substrate analogue that will allow further exploration of structure and dynamics within the nucleotide binding domains of this important enzyme.

P-glycoprotein (P-gp)[1] belongs to the ATP binding cassette (ABC) superfamily of membrane transporters that are involved in the import and export of numerous compounds across cellular membranes (for reviews, see refs *1*−*3*). P-gp has drawn considerable interest because of its role in invoking multidrug resistance to anticancer and anti-AIDS therapies.

P-gp shows the typical ABC transporter domain arrangement consisting of two transmembrane domains (TMD) and two nucleotide binding domains (NBD). The TMD are predicted to span the membrane multiple times in the form of α-helices and are thought to contain two positively cooperative drug binding sites, with different but overlapping specificities (*4*, *5*). The NBD may be viewed as molecular motors that transform the chemical potential energy of ATP into conformational changes of the protein. They contain the highly conserved Walker A and B consensus motifs for nucleotide binding and the "LSGGQ" motif, which is the diagnostic signature sequence of ABC proteins.

Studies using vanadate trapping experiments led to considerable insight into the catalytic cycle of P-gp. The first mechanistic model for drug transport (*6*) proposed an alternating site mechanism in which the two nucleotide binding sites cooperate and alternately carry out ATP hydrolysis, with the collapse of the chemical transition state and release of ADP and P_i providing the driving force for drug export via coupled long-range conformational changes between the NBD and the transmembrane domains. Strong evidence for this model came from experiments showing that extensive cross-communication between the different subdomains is essential to the protein function and regulation. Indeed, the presence of transport substrate greatly stimulates the protein ATPase activity, indicating that ATP hydrolysis and drug transport are coupled. Further evidence for the communication between the two NBD came from elegant experiments in which the NH_2- and COOH-terminal halves

† This work was supported by a grant from the SMU University Research Council to P.D.V. and NIH Grant GM50156 to A.E.S.

* To whom correspondence should be addressed. Phone: 214-768-1790. Fax: 214-768-3955. E-mail: pvogel@mail.smu.edu.

§ Southern Methodist University.

‡ Texas Tech University Health Science Center.

University of Rochester Medical Center.

[1] Abbreviations: ESR, electron spin resonance spectroscopy; P-gp, P-glycoprotein; Cys-less P-gp, a mutant form of P-glycoprotein in which all naturally occurring cysteine amino acids were replaced by alanine; SL-ATP, 2′,3′-(2,2,5,5,-tetramethyl-3-pyrroline-1-oxyl-3-carboxylic acid ester) ATP, 2′,3′ indicates a rapid equilibrium of the ester bond between the 2′ and 3′ hydroxyl of ATP; NBD, nucleotide binding domain; TMD, transmembrane domain.

10.1021/bi0512445 CCC: $30.25
Published on Web 10/01/2005

of the protein were expressed as separate polypeptides. Both halves showed low level of basal ATPase activity (*7*), which suggested that both NBD could hydrolyze ATP. However, the transport-substrate-stimulated ATPase activity was only observed when both halves were coexpressed, demonstrating that interactions between the two halves of the transporter are critical to its function. Supporting evidence for cooperation between the two NBD came from experiments showing that mutations in the Walker A motif of either NBD1 or NBD2 (*8*), vanadate trapping at one site (*9*) or NEM modification of one NBD (*10*) are sufficient to abolish ATPase activity at both sites. Furthermore, while the two NBD show highly cooperative inhibition in trapping experiments, the kinetics of ATP hydrolysis is strictly Michaelis−Menten (*11*, *12*), in keeping with the proposal that only one site is catalytically active at any point in time.

More recently, biochemical studies (*13*−*15*) as well as the crystal structural models of Rad50 (*16*), MJ0796 (*17*), EcMalK (*18*), and most recently MsbA (*19*) suggested the existence of a "nucleotide-sandwich" dimer where the two NBD dimerize and interdigitate with ATP bound along the dimer interface flanked by the Walker A of one subunit and the LSGGQ motif of the other to form an integrated single entity containing two bound ATP (closed conformation). Just one of the two bound ATP is hydrolyzed per dimerization event. In this modified model, formation and dissociation of the NBD dimer upon ATP binding and hydrolysis provide a regulated switch that induces conformational changes in the TMD to mediate transport. The available data seem to suggest that binding of the transport substrate to the TMD initiates the transport cycle by transmitting a conformational change to the NBD, enhancing the binding of ATP, and lowering the activation energy for closed dimer formation. ADP dissociation from the transition state seems to be favored upon nucleotide hydrolysis.

Determining the stoichiometry and characteristics for ATP binding to the different states of P-gp is a key element in validating this model. Binding of ATP to the protein is rather weak as evidenced by the K_m (MgATP) of 0.4 to 1.4 mM (*20*, *21*), which made it difficult to measure binding affinities under equilibrium conditions. Binding studies using a fluorescent analogue of ATP, TNP-ATP, (*22*, *23*) indicated that two ATP bound to P-gp. The use of a fluorescently labeled P-gp, MIANS-P-gp (*24*) also suggested that two ATP bound to P-gp and for the first time established a dissociation constant for ATP to be about 300 μM. However, the fluorescently labeled protein was catalytically inactive. Data resulting from an elaborate study that tested the sensitivity of the intrinsic fluorescence of P-gp tryptophan residues to the binding of nucleotides and various drug substrates indicated a K_d for nucleotide binding between 200 and 300 μM (*25*).

In this present study, we for the first time employed an alternative biophysical technique, electron spin resonance spectroscopy (ESR) with use of spin-labeled ATP to obtain further information about structure, function, and dynamics within the nucleotide binding sites of P-gp in addition to obtaining independent data on the nucleotide binding characteristics of this important enzyme.

Spin-labeled nucleotides have been used successfully to study nucleotide binding to the nucleotide binding sites of F_1-ATPases from different species (*26*−*31*, for review see ref *32*) as well as chaperones GroEL, DnaK, and human Hsp90 (*33*−*35*), the G-protein, p21ras (*36*), and the calcium channel, RyR1 (Dias, J. M. et al., manuscript in preparation).

We have in this study utilized pure, soluble, wild-type and Cys-less mouse mdr3 P-gp[2] to assess the ATP binding stoichiometry under equilibrium conditions. We confirmed that two ATP bound to the protein in its resting state with a single K_d in the high micromolar range. We also showed that binding of the transport substrate verapamil to P-gp causes a conformational change that results in chemical reduction of the protein bound spin-labeled nucleotide. Because ESR is a very conformation sensitive technique, we were also able to show that the bound nucleotide appears to be deeply buried inside the nucleotide-binding site when trapped in a transition-like state, while binding of the nucleotide analogue in the resting state did not have a drastic effect on the conformation of the individual binding sites.

EXPERIMENTAL PROCEDURES

Construction of Cys-Less Mouse MDR3 P-Glycoprotein Gene; Incorporation of Mutant Genes in Pichia pastoris. Details of the procedure will be given elsewhere (Tombline, G., Urbatsch, I. L., and Senior, A. E., manuscript in preparation). Briefly, mutagenesis was used to replace all nine natural Cys residues present in wild-type mouse mdr3 Pgp by Ala, using either the Altered Sites II mutagenesis kit (Promega) or by PCR mutagenesis. The templates for mutagenesis were pAlt-mdr3N (*8*) and pAlt-mdr3.6C (*37*). Mutations were then transferred on suitable restriction fragments into plasmid pHIL-mdr-3.6-His6 (*37*). DNA sequencing was carried out to ensure that only the desired mutations were present in the final plasmid, which was named pHIL-mdr3.6CL-His6. For recombination of the Cys-less Pgp gene and expression in *Pichia pastoris*, the procedures described in ref *8* were followed. Several strains were found that expressed well and were saved as glycerol stocks.

Purification of P-gp. Wild-type and a cysteine-less mutant of the mouse mdr3 P-gp were expressed in *P. pastoris* and purified to near homogeneity as described previously (*8*, *22*), with some modifications as follows: *P. pastoris* was incubated in 0.5% (v/v) methanol minimal medium for 24 h. After that, the methanol concentration was increased to 1% (v/v) and the culture was incubated for an additional 24 h. The pH was adjusted to ~6.0 at 8, 24, and 30 h incubation. Crude microsome preparation as well as solubilization and purification of P-gp were as described previously (*8*, *22*), except that the time for the solubilization step with *n*-dodecyl-β-D-maltoside (Anatrace) was increased to 20 min. Binding of the histidine-tagged proteins to Ni-NTA agarose was achieved in 1 h. The DEAE-cellulose ion exchange chromatography described in ref *22* was omitted. P-gp homogeneity was estimated to be over 90% using SDS electrophoresis.

Activation of P-gp ATPase with DTT and Lipid. Activation of P-gp with DTT and lipids was essentially as described previously (*22*) except that 2−8 mM DTT and L-α-phosphatidyl-choline from soybean (~40%) (Sigma) was

[2] Mouse mdr3 P-gp is 87% identical in sequence to human P-gp.

used for reconstitution at a final ratio of 2:1 lipid/protein (w/w). For ESR measurements, P-gp was activated with 2 mM DTT at room temperature for 20 min. The Cys-less P-gp was not activated by DTT (*38*).

Assays of P-gp ATPase Activity. Routine ATPase activity measurements were performed utilizing a coupled enzyme assay (*39*). The needed amount of P-gp (10 to 30 μg) was added to 1 mL of ATPase cocktail (10 mM ATP, 12 mM $MgSO_4$, 1 mM PEP, 0.28 mM NADH, 50 mM Tris-Cl, pH 7.4, 10 mM KCl, 0.014 mg/mL lactate dehydrogenase, 0.0288 mg/mL pyruvate kinase) at 37 °C. When required, 150 μM verapamil in DMSO or DMSO alone was added. ATP hydrolysis was recorded as the absorbance decrease at 340 nm ($\epsilon = 6300\ M^{-1}\ cm^{-1}$). The ATPase activity was alternatively measured using a colorimetric determination of the P_i released during the ATP-hydrolysis reaction. The required amount of P-gp (10−30 μg) was added to 220 μL of 50 mM Tris-Cl, pH 7.5, ATP (10 mM or 200 μM) or SL-ATP (200 μM), 10 mM $MgCl_2$, and incubated at 37 °C. When needed, 150 μM verapamil in DMSO or DMSO was added. At appropriate times, 50 μL aliquots were transferred to 1 mL of ice-cold 20 mM H_2SO_4 to quench the reaction, and the colorimetric development was carried out as described (*40*).

Inhibition of P-gp ATPase by Trapping SL-Nucleotides with AlFx and BeFx. Inhibition of P-gp ATPase by trapping nucleotides with AlFx and BeFx was carried out as described in ref *8*. Different amounts of P-gp were incubated with 2 mM DTT, 2 mM $MgSO_4$, 150 μM verapamil, 1 mM SL-ATP, and 1 mM $AlCl_3$, 5 mM NaF, or, 200 μM $BeSO_4$, 1 mM NaF, and 50 mM Tris-HCl, pH 7.5 in 100 μL total volume at 37 °C for various times. Incubations were started by the addition of P-gp and stopped by transfer of the sample onto ice. Unbound, excess ligand was then removed using the centrifuge column technique (*8*, *41*).

ESR Measurement. All ESR measurements were performed using a Bruker EMX 6/1 ESR spectrometer operating in the X-band mode, equipped with a high sensitivity cavity. A total of 30 μL of sample was pipetted into a 50 μL glass calibrated capillaries. The top of the tube was closed, and it was inserted into a quartz cuvette. The measurements were made with the following constant parameters: microwave frequency: 9.33 GHz, microwave power: 12.63 mW, modulation frequency: 100 kHz, resolution: 1024 points. The 12 mW microwave power used in these experiments is within the appropriate range of 10 to 20 mW microwave power routinely used for liquid water samples. For whole spectrum measurements, the centerfield was set at 3325 G and an area of 100 G was scanned with a peak-to-peak modulation amplitude of 1 G. A time constant of 10.40 ms and a conversion time of 40.96 ms were used, giving a total sweep time of 41.943 s. The signal gain was adjusted to the SL-ATP concentrations in the different experiments. For low- and high-field measurements of the protein-bound SL-nucleotides, an area of 20 G was scanned and the modulation amplitude was increased to 2 G. The time constant was 40.96 ms and the conversion time was set to be 163.84 ms. The receiver gain was varied between 5×10^5 and 2×10^6 to give the highest signal/noise ratio. The buffer used for ESR spectroscopy was 50 mM Tris-HCl pH 7.4, 50 mM NaCl, 20% glycerol, 0.1% DM, 300 mM imidazole, 1 mM DTT (DTT was absent when Cys-less was measured) and ± 2 mM $MgSO_4$, ± 150 μM verapamil. Control experiments showed that the spin-label was not reduced by DTT during the time of the experiment. The amount of protein-bound spin-labeled nucleotide was determined as the difference between the known total concentration of spin-labeled nucleotide added to the ESR cuvette and the free spin-labeled nucleotide observed. The free nucleotide was measured directly by comparing the signal amplitude of the high field signal of the unbound nucleotide spin label to a standard curve of known concentrations of spin-labeled nucleotide that was generated under the same conditions in the absence of protein. Unless otherwise noted, all measurements were performed at room temperature. The mol of protein-bound SL-ATP per mol of protein was plotted over the concentration of free SL-ATP present and the results were fitted using the equation $y = P1*x/(P2 + x)$ for a rectangular hyperbola, where P1 represents the maximum number of binding sites and P2 represents the equilibrium dissociation constant K_d. Nonlinear curve fits were performed using Origin 7 (OriginLab Corp.).

Synthesis of SL-ATP. 2′,3′-(2,2,5,5,-Tetramethyl-3-pyrroline-1-oxyl-3-carboxylic acid ester) ATP (SL-ATP) was synthesized essentially as described (*26*, *42*), with the exception that the nucleotide analogue was purified using Sephadex DEAE-A25 anion exchange chromatography and a linear gradient of 0−0.6 M triethylammonium bicarbonate buffer, pH 7.5, and not reversed phase column chromatography as previously described.

Routine Procedures. Protein concentrations were determined by the modified Lowry procedure (*43*) using bovine serum albumin as a standard. Protein purification was assessed using 8% SDS−polyacrylamide gel electrophoresis. For immunodetection of P-gp, mouse monoclonal antibody C219 (Signet Laboratories) was used with the alkaline phosphatase colorimetric detection system.

RESULTS

ESR spectroscopy is a biophysical technique that specifically detects unpaired electrons. Because the natural occurrence of such paramagnetic species in biological systems is relatively low, ESR sensitive reporter groups (spin labels or spin probes) can be introduced chemically into biological systems, either through chemical modification of the protein or via spin-labeled substrates or cofactors. The method is highly sensitive to conformational transitions within the vicinity of these reporter groups and therefore allows the evaluation of dynamic conformational processes during substrate binding and often during enzymatic turnover. ESR is especially useful for studies of membrane proteins where many other biophysical methods are "handicapped" due to the specific characteristics of biological membranes, e.g., ESR is unaffected by light scattering, and it can also be used at high viscosities of the samples. Furthermore, the relatively small size of the spin-label usually does not perturb the biological activity of the enzyme or protein. Requirements, however, are relatively large protein amounts and rather high protein concentrations (usually >10 μM) that are needed for acceptable signal-to-noise ratio of the resulting ESR spectra. This can be difficult to obtain, especially when working with membrane proteins. The development of the *P. pastoris* expression system allows the expression of fully functional

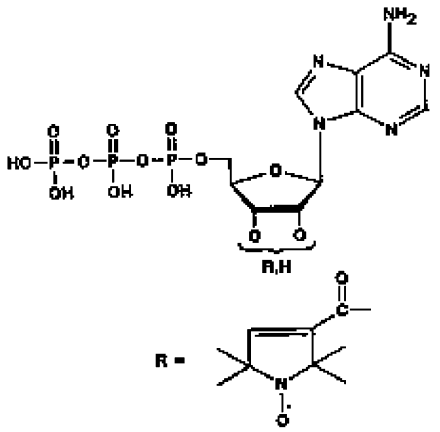

FIGURE 1: Spin-labeled ATP-analogue: 2′,3′-(2,2,5,5,-tetramethyl-3-pyrroline-1-oxyl-3-carboxylic acid ester) ATP (2′,3′ indicates a rapid equilibrium of the ester bond between the C2′ and C3′).

P-glycoprotein at yields that are adequate for ESR spectroscopy (*22*), therefore allowing the use of this powerful biophysical technique to study this enzyme.

In the present work, mouse wild-type and Cys-less mdr3 P-gp were purified to near homogeneity from *P. pastoris* cells by employing nickel-NTA-affinity chromatography. The detergent-soluble enzymes were shown to be active ATPases. ATP hydrolysis activity was readily activated by the transport substrate verapamil (*22*).

In earlier studies to evaluate the binding characteristics of P-gp, fluorescence spectroscopy was used, either employing fluorescent nucleotide analogues, fluorescently labeled P-gp, or the naturally occurring fluorescence due to tryptophan residues in the enzyme (*22*−*25*).

In this study, we employed an alternate, not fluorescence spectroscopy based approach, namely, ESR spectroscopy, to study nucleotide binding to P-gp. This method allowed us to directly measure the binding of substrate analogues to the enzyme while giving additional information about the environment of the reporter group. We used a spin-labeled ATP analogue, 2′,3′-(2,2,5,5,-tetramethyl-3-pyrroline-1-oxyl-3-carboxylic acid ester) ATP (SL-ATP) (Figure 1), which contains a stable nitroxide radical attached to the 2′,3′ position of the ribose. This analogue has been successfully used in previous studies to investigate a variety of different nucleotide binding proteins (*26*−*31*, *35*).

SL-ATP Is an Excellent Substrate Analogue to Study ATP-Binding to P-gp. Drug-stimulated ATPase activity of SL-ATP was observed to be ∼14% of that determined for normal ATP at the same concentration. The specific activities were determined at 200 μM ATP or SL-ATP using a colorimetric assay that determines P_i-formation. A specific activity of 30.9 nmol/min/mg was observed in the presence of 200 μM ATP, compared to 4.4 nmol/min/mg in the presence of 200 μM SL-ATP. Under V_{max} conditions (10 mM ATP), our protein preparations resulted in specific activities of about 480 nmol/min/mg. The somewhat smaller activities observed for ATP-hydrolysis in our experiments than those previously published may be due to the different lipid composition and the different lipid: protein ratio that we used in our experiments. No basal ATPase activity was detected at 37 °C at 200 μM SL-ATP or ATP.

When incubated with SL-ATP, Mg^{2+}, verapamil, and AlF_x or BeF_x, P-gp was efficiently trapped in reversibly inhibited

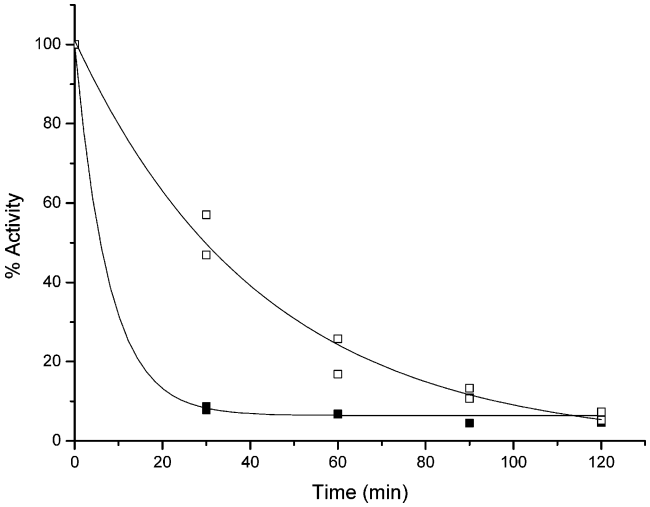

FIGURE 2: Inhibition of the ATPase activity of wild-type P-glycoprotein upon preincubation with AlFx and MgSL-ATP or BeFx and MgSL-ATP. P-gp was incubated with 2 mM DTT, 150 μM verapamil, 2 mM $MgSO_4$, 1 mM $AlCl_3$, 5 mM NaF or 200 μM $BeSO_4$ and 1 mM NaF and 1.37 mM SL-ATP in 50 mM TrisCl (pH 7.5) at 37 °C (*8*). At the times indicated, aliquots were taken and passed through a spin column (*41*). The ATPase activity was determined using a coupled enzyme assay (*39*). The solid line is a fit to the exponential equation $y = A1^{(-x/t1)} + y_0$, (■) AlFx, (□) BeFx.

conformations, see Figure 2, that are thought to mimic the transition and resting states of the protein, respectively. In both cases, the residual ATPase activity (measured with normal ATP under V_{max} conditions) was less than 10% after 120 min incubation. The AlFx-trapped P-gp was observed to reactivate after 5−10 min incubation at 37 °C.

Both the comparable ATP-hydrolysis activities (if one considers that a roughly 6-fold reduction of ATP-hydrolysis is negligible compared to the $\sim 10^9$-fold acceleration of ATP hydrolysis by P-gp) and the ability to allow similar conformational transitions within the protein (formation of transition state structures) support the fact that SL-ATP with the spin-label attached to the ribose is an excellent analogue of ATP to study nucleotide binding and structure−function of the P-gp.

SL-ATP Binding to Wild-Type P-gp under Equilibrium Conditions. Titration experiments using incrementally increasing concentrations of SL-ATP allowed us to directly follow SL-ATP binding to P-gp under equilibrium conditions. ESR spectroscopy is an especially useful tool to study relatively weak binding interactions under equilibrium conditions. The technique can be used up to almost millimolar substrate concentration because the spectral line-shape of the freely tumbling, unbound radical is distinctly different from that of the enzyme-bound component. This allows the experimentalist to observe both free and bound ligand simultaneously and under equilibrium conditions. The amount of protein-bound spin-labeled nucleotide is determined as the difference between the known total concentration of spin-labeled nucleotide added to the ESR cuvette and the free spin-labeled nucleotide observed in the experiment. The free SL-nucleotide is measured directly by comparing the signal amplitude of the high field signal of the unbound spin-labeled nucleotide to a standard curve of known concentrations of spin-labeled nucleotide that was generated in the absence of protein.

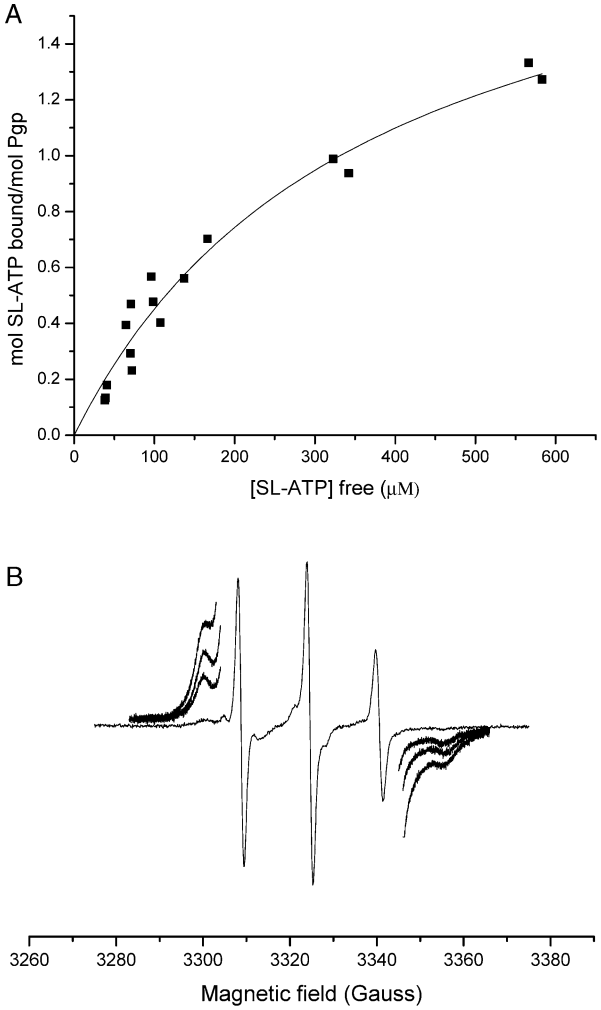

FIGURE 3: SL-ATP binding to wild-type P-gp in the presence of 2 mM Mg^{2+}: (A) 70 to 90 μM P-gp were titrated with 2′,3′-SL-ATP. The mol of protein-bound nucleotide per mol of protein was plotted over the concentrations of free SL-ATP that were determined from the corresponding ESR-spectra. Hyperbolic curve fit resulted in a maximum binding of 2.1 (± 0.2) mol/mol and a dissociation constant of 366 (± 66) μM. (B) ESR-spectra of SL-ATP binding to P-gp. Full spectrum: 92 μM P-gp in the presence of 47 μM SL-ATP. The signals of the bound component can be seen in the low and high field in the presence of 47, 91, and 190 μM SL-ATP; the spectra were re-recorded at higher signal gain for better visualization.

Using this technique, we were able to show that SL-ATP readily bound to P-gp. Figure 3A shows a binding curve generated in the presence of 2 mM Mg^{2+}. Nonlinear, hyperbolic curve fit analysis of the results extrapolated to maximum binding of 2.1 mol (± 0.2) SL-ATP per mol of P-gp and an apparent K_d of 366 μM (± 66 μM). This value is very close to the K_m measured for ATP hydrolysis (0.4 mM) (*21*) and to the K_d reported previously for binding of "normal" adenine nucleotides (*24*, *25*). The spin-labeled ATP bound to P-gp could be fully displaced by addition of excess MgATP, indicating the specificity of binding to the nucleotide-binding sites is not determined by the spin-label moiety.

Figure 3B shows the corresponding ESR spectra of SL-ATP bound to P-gp. The ESR spectrum of substoichiometric amounts of SL-ATP in the presence of P-gp is shown in full. The broad signals in the low and high field regions stem from the protein-bound SL-nucleotides. The three much more pronounced, sharp signals correspond to the free, unbound SL-nucleotides. Since the signals of the free components are much more intense than the ones corresponding to the protein-bound radicals, as is typical for all such ESR experiments, we re-recorded the signals of the protein-bound SL-nucleotide component at higher signal gain for better visualization. These re-recorded spectra can be seen as the broad signals in the low and the high field of the spectra. The signals for the "bound" spectral component were normalized for their signal gain for better comparison. The SL-ATP concentrations for the different spectra are given in the figure legend. It is evident that binding of SL-ATP to P-gp is concentration-dependent, as the intensities of the protein-bound SL-ATP signals increase with increasing SL-ATP concentrations.

The outermost splitting of the signal of the bound component ($2A_{zz}$ value) of 55 to 56 G indicates relatively high mobility of the radical within the nucleotide binding site, which is suggestive of a rather open conformation of the nucleotide site.

Binding of SL-ATP to P-gp is Mg^{2+}-dependent. In experiments that were performed in the absence of Mg^{2+} and in the presence of EDTA, we observed maximal binding of 2 mol of SL-ATP per mol of P-gp, but with a much higher K_d of 650 μM (data not shown). Addition of excess Mg^{2+} increased SL-ATP-binding to the relative amounts observed when Mg^{2+} was present from the beginning.

Control experiments showed that the protein was still fully active in ATPase assays after a standard ESR experiment. Further controls showed that the spin label was not reduced during the course of an ESR experiment by the DTT that was added to the sample to keep P-gp in its reduced state.

Effect of Verapamil on SL-ATP Binding. To analyze the effect of the transport substrate, verapamil, on the ATP binding characteristics, we titrated P-gp with SL-ATP in the presence of 2 mM Mg^{2+} and 150 μM verapamil, which was observed to be optimal for stimulation of ATPase activity of P-gp (*21*). Binding of SL-ATP to P-gp in the presence of the transport substrate verapamil resulted in surprising findings. The data are shown in Figure 4A. Even though the experimental conditions were identical to those described for the experiments in Figure 3A (except for the presence of verapamil), maximal binding and apparent K_d differed significantly from the previous data. The binding curve extrapolated to a maximum binding of about 7 mol/mol and a K_d of 680 μM.

One possible explanation for this unexpected result is that in the presence of verapamil the cysteines in the Walker A motif, which are the only exposed cysteines within P-gp (*8*, *9*, *44*) undergo a conformational transition and come into close contact with the radical moiety of the spin-label, resulting in a chemical reduction of the radical moiety. Chemical reduction of the nitroxide radical would result in the formation of an ESR-inactive hydroxylamine species as well as an ESR-silent sulfur-radical stemming from the cysteine. It is assumed that the solvent-exposed sulfur radicals would then be rapidly reduced in the presence of excess DTT to again form sulfhydryls. This process would lead to a decrease of signal amplitude of the ESR spectra. A decrease of the signal amplitude of the free component would mimic binding of the analogue to P-gp (i.e., less signal amplitude is observed than is expected when compared to the standard curve).

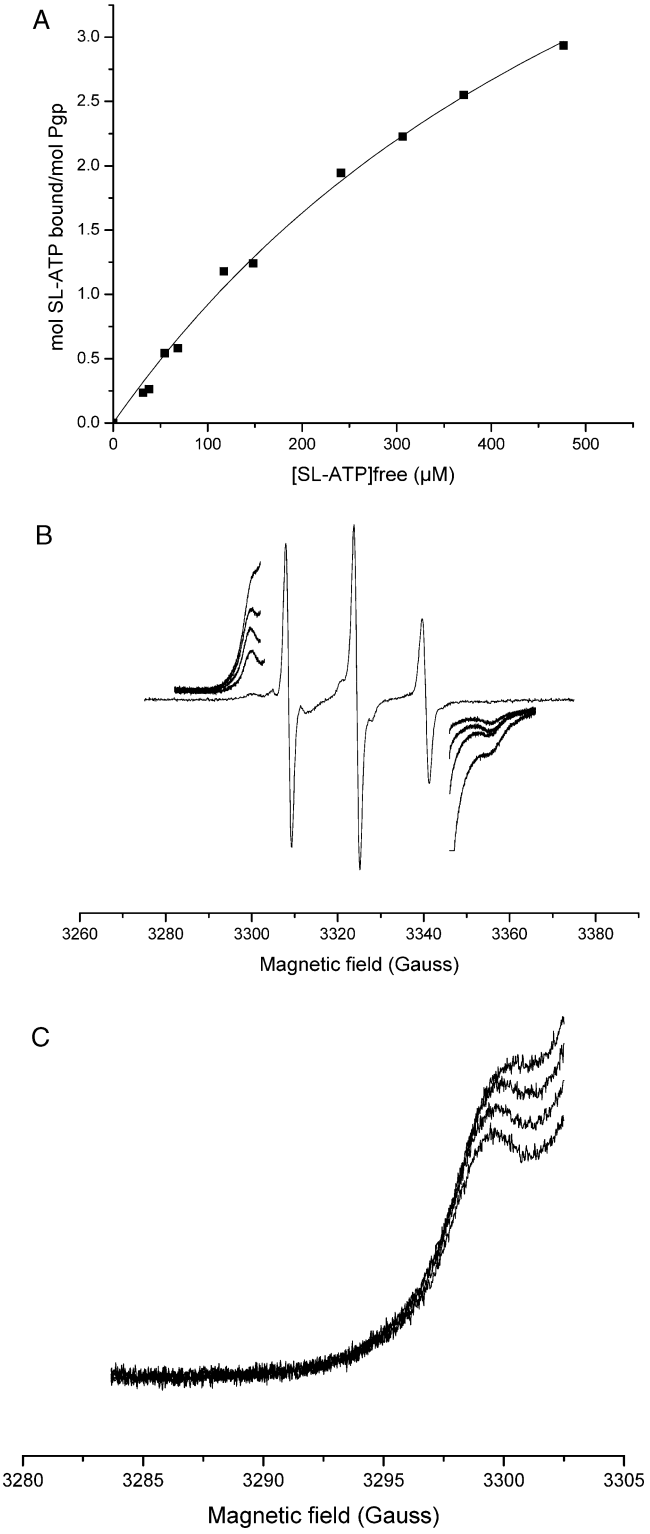

FIGURE 4: SL-ATP binding to wild-type P-gp in the presence of 2 mM Mg^{2+} and 150 μM verapamil. (A) The experimental setup was identical to Figure 3, except that 150 μM verapamil was added. Nonlinear curve analysis indicated maximum binding of 7 mol/mol and a K_d of 680 μM. (B) ESR-spectra of SL-ATP binding to P-gp: Full spectrum: 104 μM P-gp in the presence of 54 μM SL-ATP or in the presence of 54, 106, 220, and 406 μM SL-ATP. (C) Reduction of the protein-bound spin-label over time: 100 μM P-gp in the presence of 172 μM SL-ATP. The signals of the bound components were recorded over 100 min. Low field signals recorded at 0, 19, 41, and 71 min are shown here from top to bottom, respectively. The loss of signal amplitude over time was also observed for the high field signals.

Figure 4B shows the ESR-spectra of SL-ATP in the presence of P-gp and verapamil. The signals of the protein-bound SL-nucleotide component are clearly visible and increase with increasing SL-ATP concentration, confirming that binding of SL-ATP in the presence of verapamil had taken place. If a chemical reduction of the protein-bound radical took place due to the action of cysteine residues in close vicinity to the spin label, this should also be observed for the signal of the protein bound spin-labeled nucleotide. Indeed, as can be observed from the spectra in Figure 4C, the signals of the protein-bound component do decrease over time (about 25% over the time course of the experiment). Such effects were not detected in the absence of verapamil.

The data strongly suggest that this chemical reduction of the spin-labeled is due to a conformational transition within the enzyme that brings cysteines into close vicinity of the label. Since we observed hydrolysis of SL-ATP only in the presence of verapamil, it seems that either binding of verapamil or catalytic turnover of P-gp caused the conformational change to occur.

Interestingly, the $2A_{ZZ}$ value of the protein-bound SL-nucleotide component itself did not change significantly in the presence of verapamil, indicating that the radical still retained significant mobility within the binding site, in other words, the binding site was still rather open in structure after binding of verapamil.

SL-ATP Binding to Cys-less P-gp. To investigate the assumption that the protein-bound spin-label was reduced by cysteines residing in P-gp, most likely the accessible cysteines in the Walker A motifs, and that conformational transitions brought those cysteines into close contact with the radical, we reproduced the earlier experiments using a mutant of P-gp where all normally occurring cysteines had been replaced by alanines, Cys-less P-gp.

Figure 5A shows a series of titration experiments of SL-ATP to Cys-less P-gp in the presence of 2 mM Mg^{2+}. SL-ATP binds to Cys-less P-gp with somewhat greater affinity than to the wild-type P-gp. Nonlinear curve analysis resulted in a K_d of 223 μM ($\pm$ 43 μM) with maximum binding of 2.2 ($\pm$ 0.2) mol/mol. In Figure 5B the corresponding ESR spectra are shown. As expected, the amplitude of the protein-bound SL-ATP signal increased with increasing SL-ATP concentration. The observed $2A_{ZZ}$ value of 53 G is significantly smaller than that observed using wild-type P-gp (55−56 G), suggesting a higher mobility of the radical within the nucleotide binding site, most likely due to the smaller side chain of alanine as compared to cysteine.

Figure 6 shows the corresponding experiment in the presence of 2 mM Mg^{2+} and 150 μM verapamil. A maximum binding of 2.3 mol ($\pm$ 0.4) SL-ATP per mol of Cys-less P-gp was observed with a dissociation constant of 180 μM ($\pm$ 57 μM). The maximal binding of two SL-ATP per P-gp found in these experiments using the Cys-less enzyme in the presence of verapamil directly confirmed our hypothesis that cysteines of the wild-type P-gp (most likely those in the Walker A motif) were responsible for the chemical reduction of the spin-label, thereby mimicking increased binding of SL-nucleotides to P-gp.

Our data suggest that the affinity of P-gp for ATP increases to some extent in the presence of transport substrate. The $2A_{ZZ}$ value of the spectra for the protein-bound SL-ANP remained 53 G in the presence of verapamil, again indicating

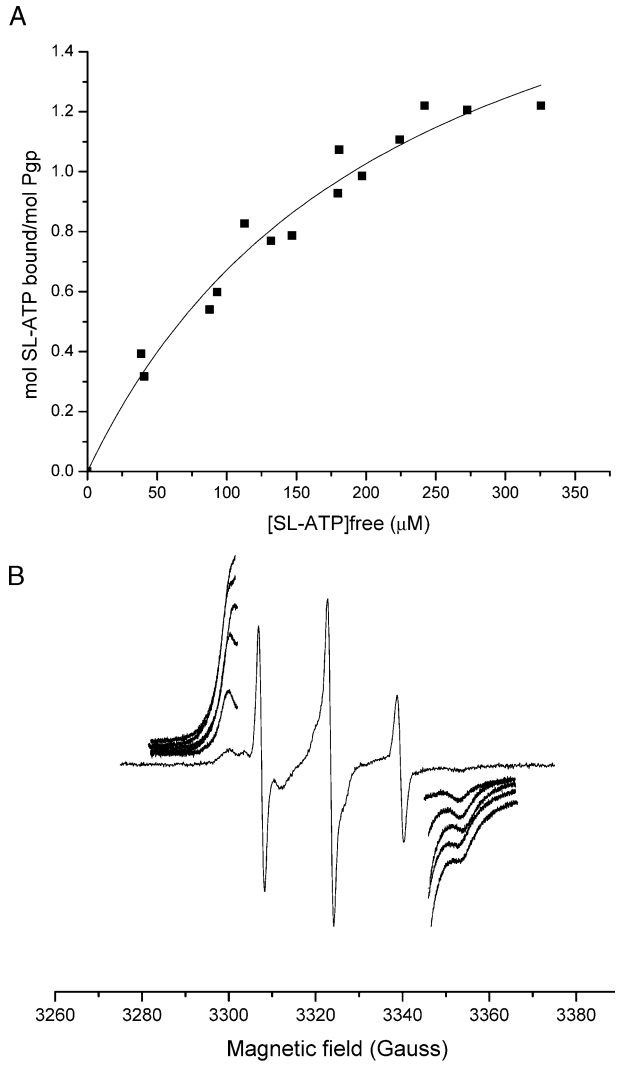

FIGURE 5: SL-ATP binding to Cys-less P-gp in the presence of 2 mM Mg^{2+}. (A) 100 to 115 μM Cys-less P-gp were titrated in the presence of 2 mM Mg^{2+}. Nonlinear curve analysis indicated maximum binding of 2.2 ($\pm$ 0.2) mol/mol and a K_d of 223 ($\pm$ 43) μM. (B) ESR-spectra of SL-ATP binding to P-gp: Full spectrum: 103 μM P-gp in the presence of 69 μM SL-ATP. The signals of the bound component are shown in the low and high field in the presence of 69, 134, 196, and 255 μM SL-ATP. The spectra were re-recorded at higher signal gain for better visualization.

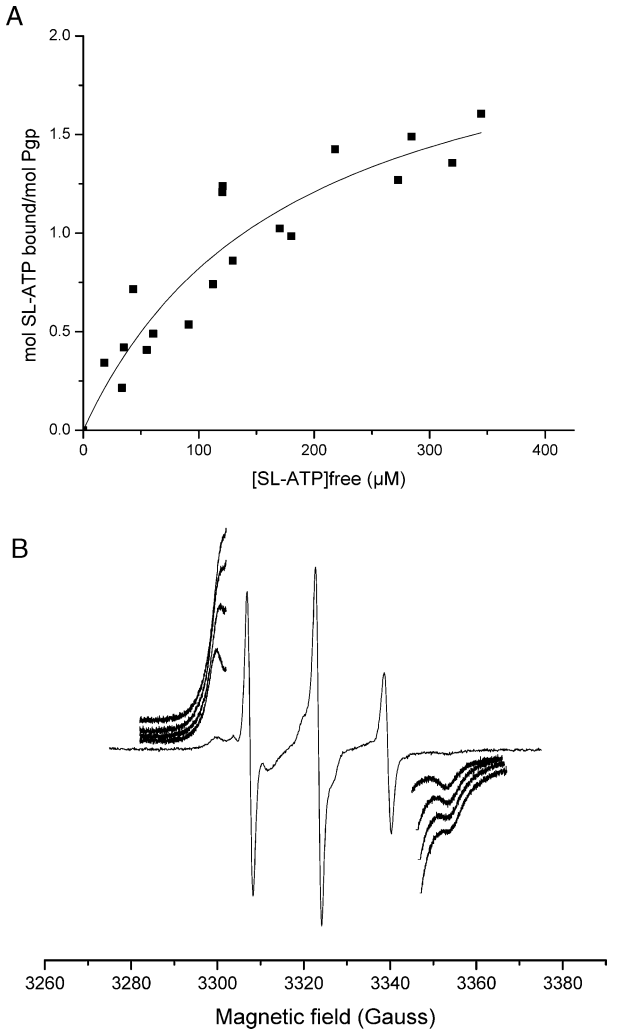

FIGURE 6: SL-ATP binding to Cys-less P-gp in the presence of 2 mM Mg^{2+} and 150 μM verapamil. (A) 80 to 100 μM of Cys-less P-gp were titrated in the presence of 2 mM Mg^{2+} and 150 μM verapamil. Nonlinear curve analysis indicated maximum binding of 2.3 ($\pm$ 0.4) mol/mol and a K_d of 180 ($\pm$57) μM. (B) ESR-spectra of SL-ATP binding to P-gp: Full spectrum: 79 μM P-gp in the presence of 82 μM SL-ATP. The signals of the bound component are shown in the presence or in the presence of 82, 161, 236, and 307 μM SL-ATP. The spectra were recorded at higher signal gain for better visualization.

that the conformational changes that seem obvious from the spin-label reduction do not directly affect the general mobility of the spin-label within the nucleotide binding sites.

ESR Observation of P-gp Closed Conformation. We used the ability of SL-ATP to be trapped in the P-gp catalytic sites by AlFx to investigate the existence of a closed conformation of P-gp. P-gp was incubated with 1 mM SL-ATP in the presence of Mg^{2+}, verapamil, and AlFx. Unbound ligand was removed by passage through a centrifuge column and the signal for SL-ATP trapped in what is assumed a hydrolysis transition state was measured using ESR at 4 °C. The lowered temperature was needed to keep the protein from reactivating.

Figure 7 shows the corresponding ESR spectra. When SL-ATP was trapped in P-gp catalytic sites with AlFx, the mobility of the spin-label decreased dramatically. The observed $2A_{ZZ}$ value of 67 G is indicative of a strongly immobilized spin-label and consistent with SL-nucleotides trapped in a closed conformation of the protein.

To ensure that the increased $2A_{ZZ}$-value was not a function of the decreased temperature, we performed similar experiments as described before with P-gp in the presence of SL-ATP, Mg^{2+} and the presence or absence of verapamil and acquired the spectra at 4 °C. In all cases, the observed $2A_{ZZ}$ for the wild-type enzyme was about 56 G (for the wild-type enzyme), the same as observed at room temperature.

The apparent absence of dipolar interaction that would result when two radicals are bound to a macromolecule in close vicinity suggests that only one SL-ATP was trapped per P-gp. It cannot, however, be excluded that two SL-ATP were bound to P-gp at a distance of more than 20 Å.

DISCUSSION

Understanding the details of the catalytic cycle of P-gp stimulated numerous studies over the past decade. Particularly, much effort was devoted to characterize the mechanisms underlying the coupling of ATPase activity and drug

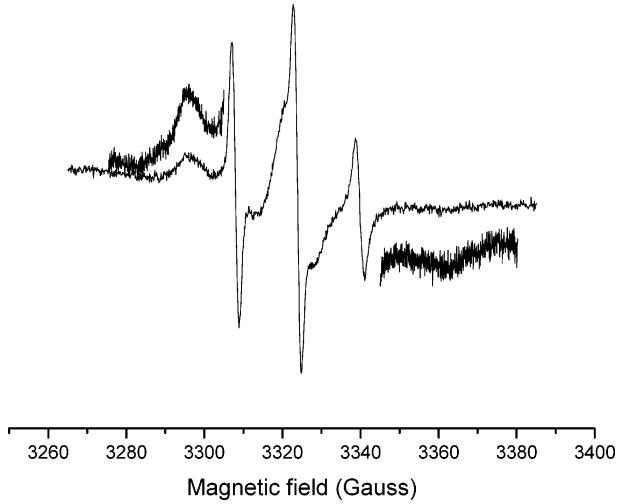

FIGURE 7: ESR spectra of wild-type P-gp with AlFx trapped SL-ATP.DTT activated wild-type P-gp was incubated with 5 mM NaF, 1 mM $AlCl_3$, 2 mM $MgSO_4$, 150 μM verapamil and 1 mM SL-ATP for 30 min at 37 °C. The unbound ligands were removed by passage through a centrifuge column and ESR spectra were measured at 4 °C. The low and high field signals were re-recorded at a higher signal gain for better visualization.

transport. A key element in the catalytic cycle of P-gp seems to be the binding of ATP and how binding of transport substrates may influence it. Recent studies have made it evident that ATP binding to the nucleotide binding sites constitutes a major event in the protein function (*2*, *3*, *45*).

Because of the weak binding affinity of P-gp for nucleotides, "traditional" equilibrium binding assays, e.g., using radioactive ATP analogues could not easily be utilized to measure binding stoichiometry and affinity. In previous studies, fluorescence spectroscopy was employed to study the nucleotide binding characteristics of P-g. Researchers used a fluorescent analogue of ATP, TNP-ATP, mostly to obtain information about the binding stoichiometry (*22*, *23*). In addition, a P-gp mutant protein that was fluorescently labeled in the Walker A motif, MIANS-labeled P-gp or, alternatively, the intrinsic tryptophan fluorescence of naturally occurring tryptophan residues was utilized to gain insight into the binding characteristics (*24*, *25*). While TNP-ATP is not a very good analogue to obtain valid dissociation constants due to strong interaction of the aromatic trinitrophenyl group with the enzyme, this analogue gave good evidence for the existence of two nucleotide binding sites on P-gp. MIANS-labeled P-gp and intrinsic tryptophan fluorescence provided comparable results for the binding affinity of adenine nucleotides binding to P-gp to be in the 200 to 400 μM range.

In this study, we used ESR spectroscopy and a spin-labeled analogue of ATP, 2′,3′-SL-ATP (SL-ATP, Figure 1), as an alternate, direct approach to investigate nucleotide binding characteristics to mouse mdr3 P-gp under equilibrium conditions. The ATP-analogue was hydrolyzed by P-gp at ~14% of the rate of "normal" ATP and could be trapped at the catalytic sites using AlFx or BeFx (Figure 2). The fully active, soluble enzyme we used therefore allowed us to directly measure ATP binding and determine the binding characteristics under enzymatic turnover conditions.

Titration experiments showed that two ATP simultaneously bound to P-gp under equilibrium conditions and in the absence or presence of transport substrate (Figures 3A, 5A, and 6A), thus bringing additional support to the model that started to emerge after the structures of MJ0796 (*17*), EcMalK (*18*), and Rad50 (*16*) with bound nucleotides were solved. The structural models show two ATP molecules binding symmetrically at the dimer interface, suggesting that two ATP must bind to form a closed dimer. The ESR spectra of the protein-bound SL-ATP exhibited only one single spectral component (Figures 3B, 5B, and 6B), indicating that both nucleotide binding sites bound to ATP with relatively symmetrical structures. This confirms that the X-ray structural models are likely to reflect the "natural" conformation of the enzyme.

All binding experiments can be satisfactorily fitted with a single K_d model equation confirming previous data (*22*, *23*). The calculated values for the dissociation constant are in the high micromolar range (200 to 400 μM), in good agreement with previous data (*24*, *25*) and the K_m for ATP hydrolysis of 0.4 mM (*21*). We also showed that the presence of Mg^{2+} increased SL-ATP binding affinity to P-gp by almost 2-fold. The K_d values for SL-ATP binding to wild-type P-gp were calculated to be 366 μM in the presence of 2 mM Mg^{2+} versus 650 μM in the absence of Mg^{2+} and in the presence of EDTA. An inverse effect of magnesium was previously reported (*22*) but seems counterintuitive as MgATP seems to be the hydrolyzed species (*21*). Also, crystal structural models of different transport ATPases show extensive interactions of the Mg^{2+} ion seemingly stabilizing the protein-bound nucleotide.

It was not possible in our experiments to determine the binding characteristics of SL-ATP to wild-type P-gp in the presence of verapamil. In the course of an experiment, the ESR signal of both the free and the enzyme bound spin-labeled nucleotide decreased, most likely as a result of chemical reduction of the spin-label under these conditions. We circumvented this problem by using a mutant of P-gp where all cysteine residues had been mutated to alanines. This Cys-less P-gp mutant showed in the presence of verapamil a slight increase in binding affinity as compared to that in the absence of verapamil. The determined K_d values for SL-ATP binding were 223 and 180 μM in the absence and presence of 150 μM verapamil, respectively. This small effect is most likely not physiologically relevant, it does, however, suggest that binding of a transport substrate directly affects the nucleotide binding sites.

The K_d values that were observed for SL-ATP-binding to the Cys-less P-gp in the absence of verapamil were about half of those observed for binding of the analogue to the wild-type protein. These differences were also mirrored in the corresponding ATP-hydrolysis assays, where we observed that the soluble Cys-less P-gp exhibited a somewhat higher ATPase activity and was slightly more activated by the addition of verapamil than wild-type P-gp. These effects may be due to less steric restriction of nucleotide binding due to the smaller alanine side chains in the mutant as compared to the normally occurring cysteines. It may also reflect the absence of even a transient disulfide bond formation between the two cysteines in the Walker motifs (even under the reducing conditions used for our experiments) that have been reported earlier.

ESR is very sensitive to conformational transitions within the environment of the reporter group. The distance between

the outermost peaks of the bound component, the $2A_{ZZ}$ value, is an excellent indicator of the relative mobility of the radical. The $2A_{ZZ}$ values of protein-bound SL-ATP (55−56 G for the wild-type and 53 G for the Cys-less) indicate a relatively mobile spin-label suggesting a very open conformation of the nucleotide binding sites. The fact that the $2A_{ZZ}$ value of SL-ANP bound to P-gp is identical in the absence and presence of verapamil indicates that no immediate conformational change had occurred in the direct vicinity of the radical that would alter its mobility. On the other hand, the observation that there is a difference in the $2A_{ZZ}$-values when the spectra of the wild-type P-gp are compared to the Cys-less mutant suggests that a cysteine side chain is located relatively close to the spin-label moiety which is positioned at the ribose of the nucleotide. Exchanging the sulfhydryl group for a proton (cysteine to alanine mutation) may result in higher mobility of the radical.

Cysteines in the Walker A motif (Cys-427 and Cys-1070 in mouse mdr3 P-gp) were shown to be the only accessible and modifiable cysteines of P-gp (*10*, *11*, *21*). Cross-linking experiments (*13*, *15*, *38*) have indicated that they can come in close vicinity from each other and from the ABC signature motif. Protection from cross-linking by ATP demonstrated that ATP is positioned close to these residues. From our results, we can assume that in the open conformation the cysteines must be positioned relatively close to the ribose group of ATP. Indeed, the reduction of the protein-bound spin-label when verapamil was present (Figure 6C) indicated that one cysteine from one Walker A motif has moved into even closer vicinity to the spin-label, resulting in direct contact with the radical and its chemical reduction. We assume that the reduction of the spin-label by the cysteine SH-group would result in formation of an ESR silent cysteine sulfur radical, which in the presence of bulk DTT would immediately be re-reduced to form cysteine. It is assumed that in the presence of excess DTT multiple such reduction−oxidation cycles were likely to happen.

In MalK (*18*), Rad50 (*16*), and MJ0796 (*17*) crystal structures, and also projected from the P-gp EM structure (*46*), the two nucleotide binding domains appear closely associated with the two ATP buried at the interface between the Walker A site of one of the nucleotide binding domains and the LSGGQ signature sequence of the second nucleotide binding domain. Contacts between the protein and the nucleotides appear extensive, with most of the contacts established between the β- and γ-phosphates of ATP, while the adenine and ribose rings do so to a lesser extent. Nonetheless, it would be expected that under these conditions the mobility of a reporter group attached to the ribose of the nucleotide would be greatly reduced.

We have investigated this closed conformation using SL-ATP that was trapped by AlFx-complex formation in what is likely similar to a transition state of hydrolysis. Excess ligand was removed by passage of the sample through a centrifuge column to allow us to observe only the trapped species. It can be assumed that due to the rather weak binding interactions between nucleotides and P-gp, most or the entire bound, but not trapped SL-nucleotide was removed under these circumstances. We found that under these conditions the radical was strongly immobilized with a $2A_{ZZ}$ value of 67 G. Such a large difference in the hyperfine splitting compared to the $2A_{ZZ}$ values observed for the resting state of the protein (56 G for the wild-type and 53 G for the Cys-less mutant) strongly indicates that a major conformational rearrangement affecting the spin-label environment had occurred, consistent with the formation of a closed dimeric structure. The ESR spectra support the findings that ATP must then be buried at the interface of the dimer, also in the soluble, not crystalline form of the enzyme.

Our results strongly support a model in which P-gp exists in two different conformations. In the resting state of P-gp the open conformation seems predominant with the nucleotide binding sites readily accessible from the aqueous phase and with a rather low binding affinity for ATP. The binding of drugs to the drug binding site(s) are likely to induce transitions that favor ATP binding (*47*) while also bringing cysteines (most likely in the Walker A motif) into close vicinity of the ribose of the bound nucleotide. A strong conformational transition then occurs when ATP is trapped in a transition-state like configuration, resulting in the nucleotide being deeply buried within the protein matrix.

We are at this time in the process of introducing single site-specific spin-labels into and close to the nucleotide binding domains of the human and mouse homologues of P-gp. Site-specific spin-labeling used in conjunction with spin-labeled nucleotides will allow us to gain further structural and dynamic information about the protein. Once two radicals are bound to the protein at relatively close distances from each other, dipolar interactions of the unpaired electrons allow us to determine the distances between these radicals. Changes within these distances upon binding of transport substrates or other activity modulating compounds can then also be monitored to a great degree of accuracy. Combining site-specific spin-labeling with the use of spin-labeled nucleotides will therefore allow us in the future to better understand the conformational dynamics of nucleotide and drug binding to this important ABC transporter protein.

ACKNOWLEDGMENT

The authors wish to thank J.G. Wise for helpful discussions.

REFERENCES

1. Holland, I. B., and Blight, M. A. (1999) ABC-ATPases, adaptable energy generators fuelling transmembrane movement of a variety of molecules in organisms from bacteria to humans, *J. Mol. Biol. 293*, 381−399.
2. Davidson, A. L., and Chen, J. (2004) ATP-binding cassette transporters in bacteria, *Annu. Rev. Biochem. 73*, 241−268.
3. Jones, P. M., and George, A. M. (2004) The ABC transporter structure and mechanism: perspectives on recent research, *Cell. Mol. Life Sci. 61*, 682−699.
4. Shapiro, A. B., and Ling, V. (1997) Positively cooperative sites for drug transport by P-glycoprotein with distinct drug specificities, *Eur. J. Biochem. 250*, 130−137.
5. Loo, T. W., Bartlett, M. C., and Clarke, D. M. (2003) Simultaneous binding of two different drugs in the binding pocket of the human multidrug resistance P-glycoprotein, *J. Biol. Chem. 278*, 39706−39710.
6. Senior, A. E., Al-Shawi, M., and Urbatsch, I. L. (1995) The catalytic cycle of P-glycoprotein, *FEBS Lett. 377*, 285−289.
7. Loo, T. W., and Clarke, D. M. (1994) Reconstitution of drug-stimulated ATPase activity following coexpression of each half of human P-glycoprotein as separate polypeptides, *J. Biol. Chem. 269*, 7750−7755.
8. Urbatsch, I. L., Gimi, K., Wilke-Mounts, S., and Senior, A. E. (2000) Conserved Walker A Ser Residues in the Catalytic Sites

of P-glycoprotein Are Critical for Catalysis and Involved Primarily at the Transition State Step, *J. Biol. Chem. 275*, 25031−25038.
9. Urbatsch, I. L., Sankaran, B., Bhagat, S., and Senior, A. E. (1995) Both P-glycoprotein nucleotide-binding sites are catalytically active *J. Biol. Chem. 270*, 26956−26961.
10. Loo, T. W., and Clarke, D. M. (1995) Covalent modification of human P-glycoprotein mutants containing a single cysteine in either nucleotide-binding fold abolishes drug-stimulated ATPase activity, *J. Biol. Chem. 270*, 22957−22961.
11. Urbatsch, I. L., Al-Shawi, M. K., and Senior, A. E. (1994) Characterization of the ATPase activity of purified Chinese hamster P-glycoprotein, *Biochemistry 33*, 7069−7076.
12. Shapiro, A. B., and Ling, V. (1994) ATPase activity of purified and reconstituted P-glycoprotein from Chinese hamster ovary cells, *J. Biol. Chem. 269*, 3745−3754.
13. Loo, T. W., Bartlett, M. C., and Clarke, D. M. (2002) The "LSGGQ" motif in each nucleotide-binding domain of human P-glycoprotein is adjacent to the opposing walker A sequence, *J. Biol. Chem. 277*, 41303−41306.
14. Urbatsch, I. L., Tyndall, G. A., Tombline, G., and Senior, A. E. (2003) P-glycoprotein catalytic mechanism: studies of the ADP-vanadate inhibited state, *J. Biol. Chem. 278*, 23171−23179.
15. Loo, T. W., Bartlett, M. C., and Clarke, D. M. (2003) Drug binding in human P-glycoprotein causes conformational changes in both nucleotide-binding domains, *J. Biol. Chem. 278*, 1575−1578.
16. Hopfner, K. P., Karcher, A., Shin, D. S., Craig, L., Arthur, L. M., Carney, J. P., and Tainer, J. A. (2000) Structural Biology of Rad50 ATPase: ATP-Driven Conformational Control in DNA Double-Strand Break Repair and the ABC-ATPase Superfamily, *Cell 101*, 789−800.
17. Smith, P. C., Karpowich, N., Millen, L., Moody, J. E., Rosen, J., Thomas, P. J., and Hunt, J. F. (2002) ATP binding to the motor domain from an ABC transporter drives formation of a nucleotide sandwich dimer, *Mol. Cell 10*, 139−149.
18. Chen, J., Lu, G., Lin, J., Davidson, A. L., and Quicho, F. A. (2003) A tweezers-like motion of the ATP-binding cassette dimer in an ABC transport cycle, *Mol. Cell 12*, 651−661.
19. Reyes, C. L., and Chang, G. (2005) Structure of the ABC transporter MsbA in complex with ADP.vanadate and lipopolysaccharide, *Science 308*, 1028−1031.
20. Al-Shawi, M. K., and Senior, A. E. (1993) Characterization of the adenosine triphosphatase activity of Chinese hamster P-glycoprotein, *J. Biol. Chem. 268*, 4197−4206.
21. Beaudet, L., Urbatsch, I. L., and Gros, P. (1998) High-level expression of mouse Mdr3 P-glycoprotein in yeast *Pichia pastoris* and characterization of ATPase activity, *Methods Enzymol. 292*, 397−413.
22. Lerner-Marmarosh, N., Gimi, K., Urbatsch, I. L., Gros, P., and Senior, A. E. (1999) Large scale purification of detergent-soluble P-glycoprotein from *Pichia pastoris* cells and characterization of nucleotide binding properties of wild-type, Walker A, and Walker B mutant proteins, *J. Biol. Chem. 274*, 34711−34718.
23. Qu, Q., Russell, P. L., and Sharom, F. J. (2003) Stoichiometry and affinity of nucleotide binding to P-glycoprotein during the catalytic cycle, *Biochemistry 42*, 1170−1177.
24. Liu, R., and Sharom, F. J. (1996) Site-Directed fluorescence Labeling of P-glycoprotein on Cysteine Residues in the Nucleotide Binding Domains, *Biochemistry 35*, 11865−11873.
25. Liu, R., Siemiarczuk, A., and Sharom, F. J. (2000) Intrinsic fluorescence of the P-glycoprotein multidrug transporter: sensitivity of tryptophan residues to binding of drugs and nucleotides, *Biochemistry 39*, 14927−14938.
26. Vogel-Claude, P., Schäfer, G., and Trommer, W. E. (1988) Synthesis of a Photoaffinity-Spin-Labeled Derivative of ATP and its First Application on F_1-ATPase, *FEBS Lett. 227*, 107−109.
27. Vogel, P. D., Nett, J. H., Sauer, H. E., Schmadel, K., Cross, R. L., and Trommer, W. E. (1992) Nucleotide-Binding Sites on Mitochondrial F_1-ATPase: Electron Spin Resonance Spectroscopy and Photolabeling by Azido-Spin-Labeled Adenine Nucleotides Support an Adenylate Kinase-Like Orientation, *J. Biol. Chem. 267*, 11982−11986.
28. Burgard, S., Nett, J. H., Sauer, H. E., Kagawa, Y., Schäfer, H. J., Wise, J. G., Vogel, P. D., and Trommer, W. E. (1994) Effects of magnesium ions on the relative conformation of nucleotide binding sites of F1-ATPases as studied by electron spin resonance spectroscopy, *J. Biol. Chem. 269*, 17815−17819.
29. Lösel, R. M., Erbse, A. H., Nett, J. H., Wise, J. G., Berger, G., Girault, G., and Vogel, P. D. (1996) Investigating the Structure of Nucleotide Binding Sites on the Chloroplast F_1-ATPase Using ESR−Spectroscopy, *Spectrochim. Acta, Part A 52*, 73−83.
30. Lösel, R. M., Wise, J. G., and Vogel, P. D. (1997) Asymmetry of catalytic but not of noncatalytic sites on *Escherichia coli* F1-ATPase in solution as observed using electron spin resonance spectroscopy, *Biochemistry 36*, 1188−1193.
31. Burgard, S., Harada, M., Kagawa, Y., Trommer, W. E., and Vogel, P. D. (2003) Association of α-subunits with nucleotide-modified β-subunits induces asymmetry in the catalytic sites of the F_1-ATPase $\alpha_3\beta_3$-hexamer, *Cell Biochem. Biophys. 39*, 175−181.
32. Vogel, P. D. (2000) Insights into ATP synthase structure and function using affinity and site-specific spin labeling, *J. Bioenerg. Biomembr. 32*, 413−421.
33. Guhr, P., Neuhofen, S., Coan, C., Wise, J. G., and Vogel, P. D. (2002) New Aspects on the Mechanism of GroEL-Assisted Protein Folding, *Biochim. Biophys. Acta 1596*, 326−335.
34. Neuhofen, S., Theyssen, H., Reinstein, J., Trommer, W. E., and Vogel, P. D. (1996) Nucleotide Binding to the Heat Shock Protein DnaK as Studied by ESR Spectroscop, *Eur. J. Biochem. 240*, 78−82.
35. Scheibel, T., Neuhofen, S., Weikl, T., Mayr, C., Reinstein, J., Vogel, P. D., and Buchner, J. (1997) ATP-binding properties of human Hsp90, *J. Biol. Chem. 272*, 18608−18613.
36. Haller, M., Hoffmann, U., Schanding, T., Goody, R. S., and Vogel, P. D. (1997) Nucleotide-Hydrolysis Dependent Conformational Changes in $p21^{ras}$ as Studied Using ESR−Spectroscopy, *J. Biol. Chem. 272*, 30103−30107.
37. Urbatsch, I. L., Gimi, K., Wilke-Mounts, S., and Senior, A. E. (2000) Investigation of the role of glutamine-471 and glutamine-1114 in the two catalytic sites of P-glycoprotein, *Biochemistry 39*, 11921−11927.
38. Urbatsch, I. L., Gimi, K., Wilke-Mounts, S., Lerner-Marmarosch, N., Rousseau, M. E., Gros, P., and Senior, A. E. (2001) Cysteines 431 and 1074 are responsible for inhibitory disulfide cross-linking between the two nucleotide-binding sites in human P-glycoprotein, *J. Biol. Chem. 276*, 26980−26987.
39. Vogel, G., and Steinhart, R. (1976) ATPase of *Escherichia coli*: purification, dissociation, and reconstitution of the active complex from the isolated subunits, *Biochemistry 15*, 208−216.
40. Van Veldhoven, P. P., and Mannaerts, G. P. (1987) Inorganic and organic phosphate measurements in the nanomolar range, *Anal. Biochem. 161*, 45−48.
41. Penefsky, H. S. (1977) Reversible binding of Pi by beef heart mitochondrial adenosine triphosphatase, *J. Biol. Chem. 252*, 2891−2899.
42. Streckenbach, B., Schwarz, D., and Repke, K. H. R. (1980) Analysis of phosphoryl transfer mechanism and catalytic centre geometries of transport ATPase by means of spin-labelled ATP, *Biochim. Biophys. Acta 601*, 34−46.
43. Peterson, G. L. (1977) A simplification of the protein assay method of Lowry et al. which is more generally applicable, *Anal. Biochem. 83*, 346−356.
44. Al-Shawi, M. K., Urbatsch, I. L., and Senior, A. E. (1994) Covalent inhibitors of P-glycoprotein ATPase activity, *J. Biol. Chem. 269*, 8986−8992.
45. Higgins, C. F., and Linton, K. J. (2004) The ATP switch model for ABC transporters, *Nat. Struct. Mol. Biol. 11*, 918−926.
46. Lee, J. Y., Urbatsch, I. L., Senior, A. E., and Wilkens, S. (2002) Projection structure of P-glycoprotein by electron microscopy, evidence for a closed conformation of the nucleotide binding domains, *J. Biol. Chem. 277*, 40125−40131.
47. Vigano, C., Julien, M., Carrier, I., Gros, P., and Ruysschaert, J. M. (2002) Structural and functional asymmetry of the nucleotide-binding domains of P-glycoprotein investigated by attenuated total reflection Fourier transform infrared spectroscopy, *J. Biol. Chem. 277*, 5008−5016.

BI0512445